Indonesian Journal of Biotechnology

VOLUME 30(2), 2025, 107-119 | RESEARCH ARTICLE

Osteogenic induction of human Wharton's jelly-derived mesenchymal stem cells using a composite scaffold from poly(ε-caprolactone) and biosilica sponge *Xestospongia testudinaria*

Andika Ardiyansyah[1], Anggraini Barlian[1,2,*], Candrani Khoirinaya[1], Sony Heru Sumarsono[1]

[1]School of Life Sciences and Technology, Institut Teknologi Bandung, Jalan Ganesha 10, Bandung 40132, Indonesia
[2]Scientific Imaging Centre, Institut Teknologi Bandung, Jalan Ganesha 10, Bandung 40132, Indonesia
*Corresponding author: aang@itb.ac.id

SUBMITTED 7 January 2025 **REVISED** 30 March 2025 **ACCEPTED** 9 May 2025

ABSTRACT Bone defects occur when bones cannot function properly due to trauma, such as accidents. In Indonesia, such defects are mainly treated by bone grafting, but the limited availability of transplants has led to the development of bone tissue engineering as an alternative. This study uses human Wharton's jelly-derived mesenchymal stem cells (hWJ-MSCs) as these can differentiate into osteoblasts when stimulated by a composite scaffold containing biosilica from the sponge *Xestospongia testudinaria*. Four main steps were performed in this study, i.e. scaffold fabrication with varying biosilica concentrations, material characterization to see whether the scaffold resembled bone tissue, hWJ-MSC isolation from the umbilical cord and cultured until passage 6, and scaffold testing to assess its compatibility and ability to support cell adhesion, proliferation, differentiation, and mineralization into bone cells. The results indicated that a scaffold with 50% biosilica has good properties for supporting hWJ-MSC growth, proliferation, and differentiation. The scaffold exhibits strong mechanical strength and hydrophilic characteristics, enhances cell proliferation, and promotes osteogenic differentiation, as confirmed by collagen type I and osteopontin expression with a higher optical density value in the Alizarin Red assay. Therefore, the 50% biosilica composite scaffold is biocompatible and osteoconductive, making it a promising candidate for bone tissue engineering.

KEYWORDS Biosilica sponge; Bone defect; Bone tissue engineering; Composite scaffold; Human Wharton's jelly-mesenchymal stem cells

1. Introduction

Bone tissue is one of the body's tissues capable of self-repair when injured or damaged. However, in patients with severe bone damage (critical-sized bone defect), the inability to self-repair can result in bone tissue loss, which subsequently reduces a person's quality of life by impairing normal activities (Nauth et al. 2018). Currently, treatment for bone defects in Indonesia still relies on the conventional bone grafting method (Taufik S et al. 2022). In bone grafting, the damaged area is transplanted with bone tissue from either the patient or a donor. A limitation of this method is the restricted supply of transplantable tissue, highlighting the need to develop alternative treatments to address this shortcoming.

Various treatments for bone defects continue to be developed. One approach that has garnered significant attention is regenerative treatment using mesenchymal stem cells (Kangari et al. 2020). Mesenchymal stem cells have been successfully applied in regenerative therapies for many years due to their multipotent capacity to differentiate into specific mature cell types, including bone cells (Caplan 2007; Marino et al. 2019). Human Wharton's jelly (hWJ) stem cells are an example of mesenchymal stem cells derived from umbilical cord tissue. Through bone tissue engineering, human Wharton's jelly-derived mesenchymal stem cells (hWJ-MSCs) can be manipulated to become bone cells using a scaffold to repair and restore the biological function of damaged bone tissue (Chaparro and Linero 2016).

The differentiation of stem cells into bone cells involves several stages, including pre-osteoblasts, immature osteoblasts, mature osteoblasts, and osteocytes. When stem cells have differentiated to the mature osteoblast stage, they serve as indicators to assess the success of bone tissue engineering (Giuliani et al. 2013). During the stem cell differentiation process, scaffolds play a crucial role in maintaining cell viability and guiding cell behavior to form new bone tissue. To fulfill this role, scaffolds must be compatible with cells, have bone-like material characteristics to support cell growth, and exhibit osteo-inductive

properties (O'Brien 2011). These parameters and characteristics depend on the materials used in scaffold construction. In line with the use of scaffolds for bone tissue engineering, research focusing on biomaterials to facilitate osteogenic proliferation and differentiation has become a prominent area of current study (Lin et al. 2020).

Composite scaffolds composed of two or more materials are continually being developed through various fabrication methods. Biosilica derived from sponges is one source of natural material that can be used in bone tissue engineering. Biosilica belongs to the bioglass group, which is inert, biocompatible, osteoconductive, and has a suitable degradation rate for scaffold construction (de Almeida Cruz et al. 2020). Sponge-derived biosilica needs to be combined with other materials, such as synthetic polymers, to create an artificial environment that mimics bone tissue (biomimetic design) and to enhance scaffold performance in facilitating new tissue formation (Qu et al. 2019). One of the synthetic polymers commonly used for bone tissue engineering is poly(ε-caprolactone) (PCL). PCL is biocompatible but not osteo-inductive, so a combination of biosilica and PCL is needed to meet the ideal parameters of composite scaffolds used in bone tissue engineering (O'Brien 2011; Cao et al. 2020).

Indonesia is known to have abundant sponge resources (Rieuwpassa and Balansa 2022; Hadi et al. 2018), particularly in the Sangihe Islands of North Sulawesi Province. One type of sponge cultivated by the local community in the Sangihe Islands is *Xestospongia testudinaria*. In biomedical applications, biosilica from the *Xestospongia testudinaria* sponge has been used for drug delivery systems and biosensors. In addition, in bone tissue engineering, biosilica can increase the expression of osteogenic genes, such as *Runx2*, alkaline phosphatase (*ALP*), osteocalcin (*OCN*), and osteopontin (*OPN*), which play a role in bone formation and mineralization (Thiagarajan et al. 2017; Mori et al. 2011). The abundant amount of *Xestospongia testudinaria* sponge can be utilized for bone tissue engineering research using a composite scaffold consisting of biosilica from *Xestospongia testudinaria* and synthetic polymer PCL. A combination of biosilica and PCL is needed to determine the potential of various concentrations of biosilica in inducing hWJ-MSC differentiation into bone cells.

2. Materials and Methods

2.1. Chemicals

All chemicals were obtained from Sigma-Aldrich Co. LLC. (St. Louis, MO, USA) unless otherwise stated.

2.2. Scaffold fabrication

The sponge *Xestospongia testudinaria* came from the Tahuna Waters of the Sangihe Islands, North Sulawesi Province. The cultivated sponges were then taken to Bandung City, West Java Province. Biosilica were extracted from the cultivated sponge and fabricated with PCL (average Mw ~14,000, average Mn ~10,000 by GPC) to form a composite scaffold. The scaffold fabrication process was carried out at the Institut Teknologi Bandung (ITB). Prior to fabrication, biosilica must be extracted from the sponge *Xestospongia testudinaria* using the calcination method adapted from Dudik et al. (2021). After cutting the sponge into small pieces weighing about 60 g, it was cleaned with distilled water to get rid of the contamination, then dried at 60 °C overnight in the oven to remove water content in the sponge and inserted in a muffle furnace for 4 h at 600 °C to vaporize the organic components in the sponge, until remain only the inorganic component.

After the calcination process, not onlybiosilica presents in inorganic component However, according to Barros et al. (2014), biosilica is the most abundant inorganic components, so the extract can be directly used to make scaffolds. The extracted biosilica was then fabricated with PCL to form a composite scaffold. The composite scaffold was fabricated using a modified salt-leaching method based on previous studies (Cannillo et al. 2010; Shaltooki et al. 2019). The salt-leaching method is a widely used technique for fabricating porous materials, especially scaffolds for tissue engineering. This method involved the use of salt particles as a pore-forming agent (porogen) to create a porous structure within a polymer or other material. As much as 10 g of PCL polymer was dissolved in 100 mL of chloroform (Merck, 102445) for 2 h. After 2 h, the dissolved PCL polymer was combined with NaCl (Merck, 3534976) with a diameter of approximately 0.25 mm, amounting to 75% of the total weight of PCL, and biosilica according to the concentration variations of 20, 30, and 50% of the total weight of PCL. The mixture was stirred with a magnetic stirrer on a hot plate for 2 h at room temperature (20–25 °C) and a speed of 500 rpm. Once homogenous, the solution was poured into a mold and further mixed with a spatula until the entire solution is in the mold.

The scaffold mixture in the mold was then allowed to dry for 2 d in a fume hood at room temperature (20–25 °C) to evaporate the chloroform solvent. The NaCl salt in the scaffold was dissolved in a 1 M NaOH (Merck, 106498) solution and incubated for 2 d in a shaker incubator at 37 °C and 150 rpm. The scaffold was then soaked in dH_2O for 1 week to remove all NaCl particles (salt-leaching). Before use, the scaffold was cut into 3 × 3 × 3 mm^3 pieces using a scalpel and liquid nitrogen. Four types of scaffold variations were used: PCL alone as a negative control and PCL combined with 20, 30, and 50% of biosilica concentrations.

2.3. Material characterization

The fabricated scaffold was then characterized by using five types of tests, including: (i) scaffold morphology observation via SEM (scanning electron microscope) and micro-computed tomography (micro-CT), (ii) identification of chemical groups through FTIR analysis, (iii) compressive strength testing to measure the scaffold's mechanical strength, (iv) water contact angle measurement

to determine surface hydrophilicity, and (v) water uptake testing to assess the scaffold's water absorption capacity. These characterizations aimed to determine whether the scaffold meets biomimetic design parameters, which mimic the characteristics of bone tissue (Huang et al. 2020).

The scaffold morphology was observed using an SEM SU3500 at the Research Center for Nanoscience and Nanotechnology ITB and using µ-CT Scanner SkyScan 1173 High-Energy micro-CT at the Basic Science Centre A ITB. The samples were coated with a gold conductive layer before SEM observation to enhance image quality. Gold enhances the emission of secondary electrons, resulting in higher contrast, sharper images, and better surface detail resolution. FTIR and compressive strength tests were conducted in the Metallurgy and Materials Engineering Laboratory, Faculty of Mechanical and Aerospace Engineering, ITB. FTIR test used Bruker Vertex 70 meanwhile compressive strength used Instron 5985 machine. The next characterization test, water contact angle measurement was performed in the Internal Combustion Engine and Propulsion Systems Laboratory, Faculty of Mechanical and Aerospace Engineering, ITB, using a Dino-Lite digital microscope. After being cut into 3 × 3 × 3 mm^3 pieces, the scaffold was immediately tested using micro-CT, FTIR, compressive strength, and water contact angle.

Micro-CT and FTIR tests utilize radiation in the testing process. The micro-CT tool used X-rays, while FTIR used infrared rays. The rays emitted by the scaffold sample will be captured by the detector for further processing. The compressive strength test was conducted to determine the pressure that can be hold by the scaffold before breaking or deforming. The scaffold will be loaded gradually at a certain speed until it experiences significant damage or deformation. The water contact angle test was carried out by dripping 3 µL of distilled water onto the scaffold surface, and the angle formed on the distilled water was measured using ImageJ software. The water uptake (WU) test was conducted in the Animal Structure and Development Laboratory, School of Life Sciences and Technology, ITB. On day 0, the scaffold was weighed and placed in a water-contained well plate until it soak. On day 1, the scaffold was weighed again and returned to the water. This process was repeated on day 2 until there was no weight gain.

$$WU\ (\%) = \frac{W_{wet}\ (g) - W_{dry}\ (g)}{W_{dry}\ (g)} \times 100\% \qquad (1)$$

WU representing water uptake and W representing the weight of the scaffold in grams (g).

2.4. Isolation and Culture of hWJ-MSCs

This research was approved by the Institutional Review Board of the Faculty of Medicine, Universitas Gadjah Mada (UGM), Yogyakarta, for the collection of human umbilical cord tissue (KE-FK-0868-EC-2020). The hWJ-MSCs was isolated from the umbilical cord of cesarean delivery donors and cultured using a growth medium consisting of Dulbecco's Modified Eagle Medium (DMEM) high glucose (Sigma-Aldrich, D5796), 10% Fetal Bovine Serum (Gibco, 16000044), and 1% Antibiotic-Antimycotic (Gibco, 15240096) in a humidified incubator at 37 °C with a 5% CO_2. Once the primary culture of hWJ-MSCs reached confluency, they were subcultured, cryopreserved and later used in experiment.

From passage 0 to passage 1, hWJ-MSCs require an incubation time of approximately 4 days, therefore to reach passage 6, at least 24 days of incubation time were needed after the cells taken from the umbilical cord (passage 0). The hWJ-MSCs passage 6 were seeded onto a sterile scaffold to observe their behavior through several parameters, i.e. adhesion, proliferation, differentiation, and mineralization. The scaffold (3 × 3 × 3 mm^3) was placed on a 96-well cell culture plate (NEST, 701001) and sterilized by washing using sterile phosphate buffered saline (PBS, Merck, 806552), PBS-1% Antibiotic-Antimycotic, 70% ethanol (OneMed, Indonesia), and exposed to UV radiation, respectively. PBS was used to clean debris and other materials that can cause contamination. PBS washing was performed by using as much as 100–150 µL, until it could wet the entire scaffold. The next washing was done by PBS-1% Antibiotic-Antimycotic and incubated for 15 min. The plate was washed again using PBS before soaked by 70% ethanol for 15 min. The 70% ethanol was discarded, and the scaffold was dried in the laminar air flow for 1 h with the exposure to the UV light radiation. The scaffold was sterile and can be used for treatment.

2.5. hWJ-MSCs testing on scaffold

Adhesion of hWJ-MSCs on the scaffold can be observed using SEM. A total of 100,000 hWJ-MSCs were seeded per scaffold. Samples need to be prepared following the protocol from Santana et al. (2015). This involved rinsing the samples with PBS and then fixed them in 2.5% glutaraldehyde (Grade I, 25% in H_2O, specially purified for use as an electron microscopy fixative, G5882) in 0.1 M cacodylate buffer (Sodium cacodylate trihydrate, 97068) pH 7.2–7.4 at room temperature for 90 min. Next, the samples was dehydrated by immersion in a graded ethanol series from 30% to 100%, each for 5 min. The samples were then fixed by soaking in hexamethyldisilazane (HMDS, reagent grade ≥ 99%, 440191) for 60 min and dried overnight. Finally, the samples were coated with gold before SEM observation.

Cytotoxicity and proliferation tests of hWJ-MSCs on the scaffold were conducted using the MTT (3-(4,5-dimethylthiazol-2-yl)-2,5 diphenyl tetrazolium bromide) assay (MTT-Formazan, 475989). The cytotoxicity test aimed to assess the scaffold's compatibility in supporting hWJ-MSCs growth; when compatible, the scaffold would be non-toxic to the cells. The proliferation test evaluates cell viability on the scaffold over specific time intervals. The cytotoxicity test was performed on day 3 post-seeding of hWJ-MSCs, while proliferation tests were conducted on days 1, 3, 5, 7, and 14. A total of 50,000 hWJ-MSCs were seeded per 3 × 3 × 3 mm^3 scaffold for the MTT assay.

The seeded hWJ-MSCs were incubated according to

the designated test schedule. For each well plate, an MTT solution was added into the samples in a 1:9 ratio with blank DMEM, and the samples were incubated for 4 h in a humidified incubator at 37 °C. After incubation, the MTT reagent was removed, and the samples were immersed in 150 µL of dimethyl sulfoxide (DMSO, 102931) to dissolve the formazan crystals formed during incubation. Absorbance was measured using a microplate reader at a wavelength of 595 nm.

Differentiation of hWJ-MSCs into bone cells was evaluated using immunocytochemistry (ICC). The purpose of ICC is to detect the expression of type I collagen and osteopontin, the osteogenic markers, through fluorescence staining and visualization using a confocal microscope. A total of 100,000 hWJ-MSCs were seeded per scaffold. Sample preparation involved removing the growth medium and washing the cells three times with PBS. The cells were fixed using 4% paraformaldehyde (PFA, A5533) and incubated for 20 min at room temperature. Following fixation, the samples were washed three times with a washing buffer. Hereafter, the cells were incubated for 45 min in a blocking buffer at room temperature, and the blocking buffer was discarded without further washing.

The second stage involved fluorescent staining. The cells were incubated with an unconjugated primary antibody for type I collagen (Invitrogen, MA1-26771) and osteopontin (Abcam, ab8448) for 1 h at room temperature, followed by washing. Subsequently, the cells were incubated with a conjugated secondary antibody Alexa Fluor 488 (Anti-rabbit IgG (H+L) F(ab')2 CF488A, SAB4600234) and Alexa Fluor 647 (Goat anti-mouse IgG H&L, Abcam, ab150115) for 1 h in the dark at room temperature. Before it was counterstained, the scaffold was washed three times using PBS and soaked in DAPI (Dihydrochloride,4′,6-Diamidino-2-phenylindole, 2HCl, 268298) and Rhodamine Phalloidin (Abcam, ab235138) for 5 min at room temperature, followed by washing at least three times using PBS. The fixed cells were visualized using an FV4000 laser scanning confocal microscope (Evident Scientific, Singapore). The expression of type I collagen and osteopontin was observed in hWJ-MSCs cultures grown on composite scaffolds up to day 21.

Mineral deposition, or the mineralization process occurring in hWJ-MSCs on the composite scaffold, was assessed on day 21 through Alizarin Red staining (Aung et al. 2019). The samples were fixed using 70% ethanol for 1 h at 4 °C, then rinsed with distilled water and stained with Alizarin Red for 10 min at room temperature. Excess Alizarin red dye was then discarded, and the sample was washed using deionized water. Subsequently, the absorbance of the solution was measured using a microplate reader at a wavelength of 405 nm. A total of 50,000 hWJ-MSCs were seeded per scaffold.

2.6. Statistical analysis

Statistical data analysis was performed to determine the significance of different composite scaffold compositions on the differentiation of hWJ-MSCs into bone cells. The obtained data were first tested for normality using GraphPad Prism 9 through the Anderson-Darling, D'Agostino & Pearson, and Shapiro-Wilk tests. After passing the normality tests, the data were analyzed using One-Way ANOVA and Tukey tests to identify groups that have significant mean differences. To facilitate interpretation, the results from each test were visualized in graphical form.

3. Results and Discussion

3.1. Morphological observation of the scaffold using SEM and micro-CT

Biosilica extracted from the sponge Xestospongia testudinaria was observed using SEM SU3500, along with the PCL. The composite scaffolds that were successfully fabricated were also analyzed using SEM. In Figure 1, biosilica is indicated by red arrows, while PCL is shown in green. Biosilica exhibits a needle-like morphology, in contrast to the amorphous structure of PCL. Biosilica is osteo-inductive and osteo-conductive, while PCL is biocompatible and biodegradable. The combination of these two materials meets the ideal parameters for composite scaffolds used in bone tissue engineering (O'Brien 2011; Cao et al. 2020). Furthermore, the extensive surface area of the scaffold facilitates the adhesion of hWJ-MSCs, thereby promoting both proliferation and differentiation (Barcena et al. 2024; Gandhimathi et al. 2019).

The morphology of the composite scaffold was also tested using micro-CT (Figure 2). This test was used to see the 3D structure of the composite scaffold based on X-ray scanning. The fabricated scaffold measured around $3 \times 3 \times 3$ mm^3. Based on the results of the transverse section of the scaffold, a structure resembling an observed hole was a pore. Pores on a scaffold are important because they affect nutrient and waste transfer, cell migration, and vascularization (Beniwal and Saxena 2021).

3.2. Identification of scaffold components

One of the tests used to confirm biosilica and PCL as components of the composite scaffold is FTIR (Fourier Transform Infrared Spectroscopy). FTIR is a technique for identifying the components of a material based on the functional groups of each constituent. Each molecule has a unique FTIR spectrum, akin to a fingerprint. By comparing the obtained spectrum with a reference spectrum database, the chemical groups present in a material can be identified (Alibrahim 2022).

Based on the obtained results, biosilica functional groups present in the composite scaffold have been identified. In Figure 2, biosilica exhibits peaks corresponding to asymmetric stretching of Si-O-Si bonds at 962.61-1108.33 cm^{-1} and symmetric stretching of Si-O-Si at the 742.99 cm^{-1} range of the infrared (IR) spectrum (Herth et al. 2016). In addition to identification, the FTIR test was also used to confirm the interaction between biosilica and PCL through the presence of the Si-OH functional group

from biosilica. This functional group was detected at a wavenumber of 816.88 cm^{-1} (asymmetric stretching), indicating that the type of chemical bond formed is a hydrogen bond (Herth et al. 2016; Kalkan et al. 2014; Phillipson et al. 2014). The hydrogen bond is formed because -OH from biosilica and carbonyl atoms (C=O) from PCL inter-

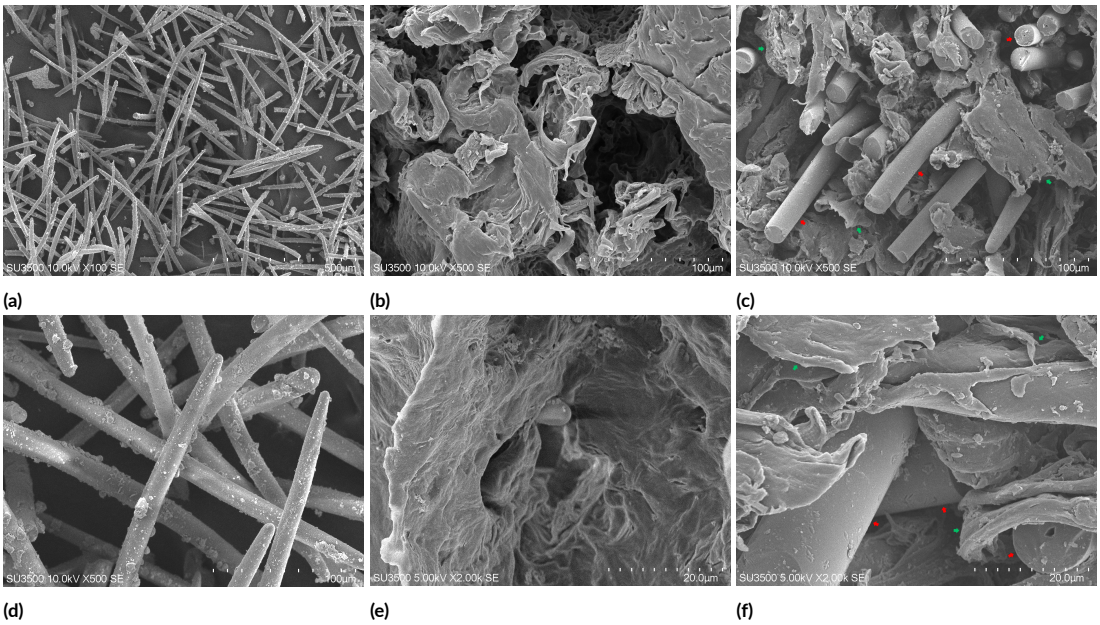

FIGURE 1 SEM observations at 100–2,000× magnification. (a) Morphology of biosilica at 100× (scale bar: 500 µm). (b) Morphology of PCL at 500× (scale bar: 100 µm). (c) Morphology of the composite scaffold contains biosilica (red arrows) and PCL (green arrows) at 500× (scale bar: 100 µm). (d) Morphology of biosilica at 500× (scale bar: 100 µm). (e) Morphology of PCL at 2,000× (scale bar 20 µm). and (f) Morphology of the composite scaffold contains biosilica (red arrows) and PCL (green arrows) at 2,000× (scale bar: 20 µm).

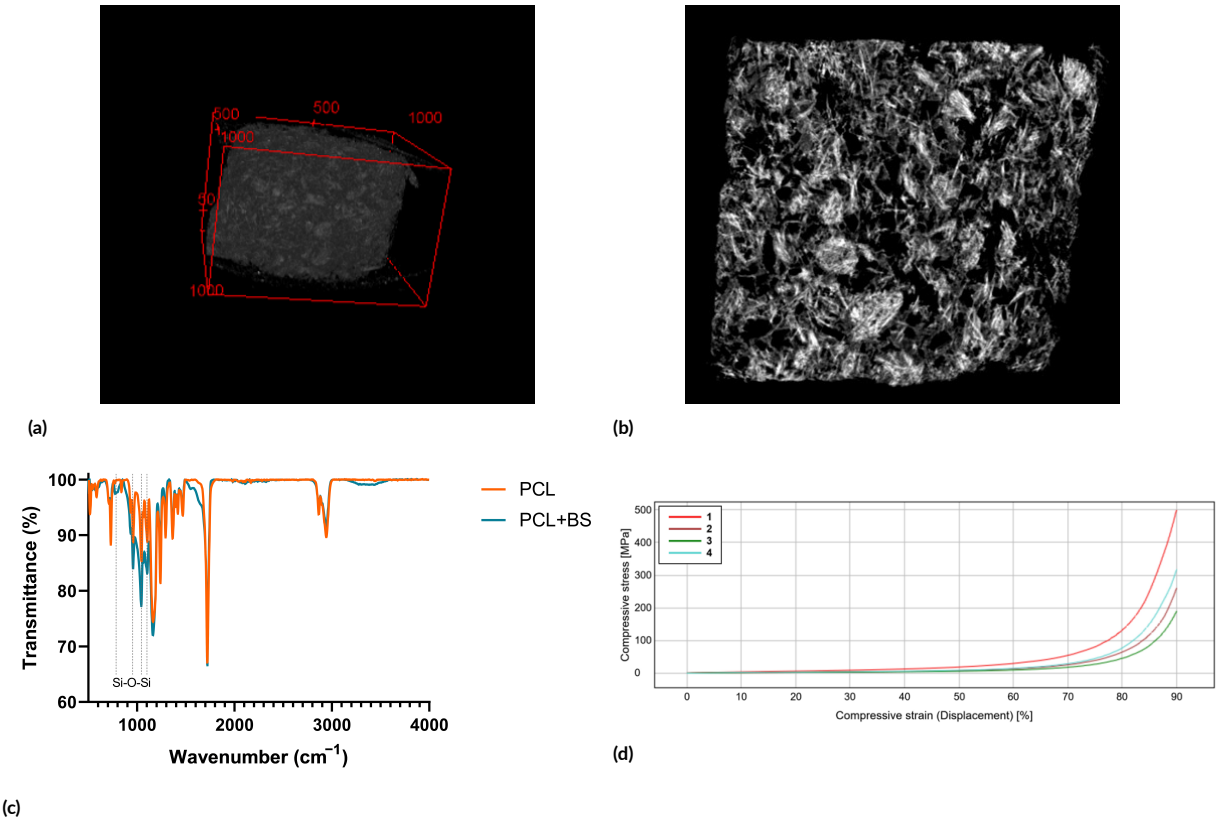

FIGURE 2 (a) 3D structure of composite scaffold. (b) Transverse section of the composite scaffold. (c) FTIR of the PCL and biosilica composite scaffold compared to the PCL scaffold. (d) Stress-strain of the compression test or mechanical strength of four variations of scaffolds. Samples 1 to 4 are PCL, PCL with 20, 30, and 50% biosilica.

act due to electrostatic attraction, making it more stable. Ultimately, the interaction between molecules through hydrogen bonds will increase the biocompatibility, thereby increasing the interaction between cells and scaffolds in the bone tissue regeneration process (Yu et al. 2022).

3.3. Mechanical strength testing of the scaffold using compressive tests

One of the parameters for scaffolds that can be applied to areas experiencing damage is having good mechanical strength, similar to bone The compressive test of the scaffolds was shown in Figure 2. PCL scaffold, represented by the bright red curve, exhibits the highest mechanical strength, indicated by a sharp increase in the curve at around 80% strain. This demonstrates that PCL has good elastic properties but begins to show a significant increase in stress as strain increases. When subjected to a pressure of 497.68 MPa, 90% of the PCL scaffold experienced damage.

According to Emadi et al. (2024), human cortical bone, which is the densest part of bone tissue, can fracture under a pressure of 240 MPa, while cancellous bone fractures at a pressure of 45 MPa. The composite scaffold with a 50% biosilica concentration exhibits higher mechanical strength compared to the 20 and 30% concentrations. This scaffold will sustain damage up to 90% when subjected to a pressure of 316.56 MPa. Compared to the study by Emadi et al. (2024), the composite scaffold with a 50% biosilica concentration is suitable for bone tissue engineering applications because it has greater mechanical strength than that of cortical bone.

In addition to mechanical strength, other parameters such as hydrophilicity characteristics are considered. Fifty percent (50%) biosilica-contained scaffold is preferred and more suitable for bone tissue engineering applications compared to PCL scaffolds, since PCL is hydrophobic, not osteoconductive, and lacks integrin binding sites to facilitate cell adhesion (Ganesh et al. 2012; Khosravi et al. 2018). Therefore, it is necessary to carry out further testing to determine the hydrophilicity characteristics of each scaffold variation.

3.4. Hydrophilicity testing of the scaffold using water contact angle

The water contact angle test was done to determine hydrophilicity of the material surface. The principle of the test is when a water droplet on the surface of a material formed an angle less than 90°, the material surface is considered hydrophilic. Conversely, when the angle is greater than 90°, the material surface is considered hydrophobic (Sundaramurthi et al. 2015).

The following are the angles formed when a water droplet is placed on the surface of the scaffold (Figure 3). The addition of biosilica lead to the scaffold to become hydrophilic. As the concentration of biosilica increases, the scaffold becomes increasingly hydrophilic. A hydrophilic scaffold surface facilitates the adhesion of hWJ-MSCs. The facilitation of cell adhesion on the scaffold surface enables the cells to proliferate. Proliferation plays a crucial role in tissue regeneration since proliferating cells can replace those that are lost due to tissue damage. Furthermore, facilitated proliferation is also correlated with optimal cell differentiation (Huang et al. 2020; Gandhimathi et al. 2019).

According to Sundaramurthi et al. (2015), when the water contact angle is below 80°, the material will stimulate cell adhesion and growth. Based on the obtained results, the composite scaffolds with 20%, 30%, and 50% biosilica concentrations have water contact angle values below 80°, indicating that composite scaffolds stimulate cell adhesion and growth compared to the PCL scaffold (Figure 3a). Among the three composite scaffolds, the one with a 50% biosilica concentration wasbetter in stimulating cell adhesion and growth. It had the smallest water contact angle value of 73.698 ± 0.256°, indicating that its surface is more hydrophilic than the others (Gandhimathi et al. 2019). The water contact angle formed on the PCL was 92.729 ± 0.15°, PCL + 20% biosilica was 79.019 ± 0.145°, and PCL + 30% biosilica scaffolds was 76.817 ± 0.263°.

3.5. Hydrophilicity testing of the scaffold using water uptake

Water uptake test was used to measure the ability of the scaffold to absorb water. This test can support the results of the water contact angle test, as it is related to the hydrophilicity characteristics of the scaffold. The water uptake test was only conducted for 2 days, as on the 3rd day, the scaffold did not experience any further increase in weight (Figure 3f). Based on the results obtained, the scaffold with a 50% biosilica concentration demonstrated the high-water absorption capacity, with the highest water absorption values on days 1 and 2. This data supported the results from the water contact angle test, where the scaffold with a 50% biosilica concentration exhibited the highest hydrophilicity. The Si-O groups in biosilica interact with water molecules (H_2O) through hydrogen bonding. As the concentration of biosilica in the scaffold increases, the presence of Si-O groups also increases, allowing for more interaction between water molecules and the scaffold (Gandhimathi et al. 2019; Sundaramurthi et al. 2015). Percentage values of the scaffold's water absorption capacity for PCL with 50% biosilica concentration are 67.62 ± 1.23% on day 1 and 75.6 ± 1.25% on day 2.

After characterization, the scaffold was then tested for biocompatibility and osteo-inductivity using hWJ-MSCs passage 6 under sterile conditions. Passage 6 is the maximum passage, the cells can be seeded onto the scaffold and after passage 6, hWJ-MSCs begin to show signs of cellular aging (senescence), leading to a decrease in their ability to divide (Facchin et al. 2018).

Biocompatibility was assessed using SEM and MTT assays, while osteo-inductivity was tested using ICC and Alizarin Red staining. Biocompatible means that scaffold is not toxic, so it can support cell attachment and proliferation. Cell attachment can be observed using the SEM

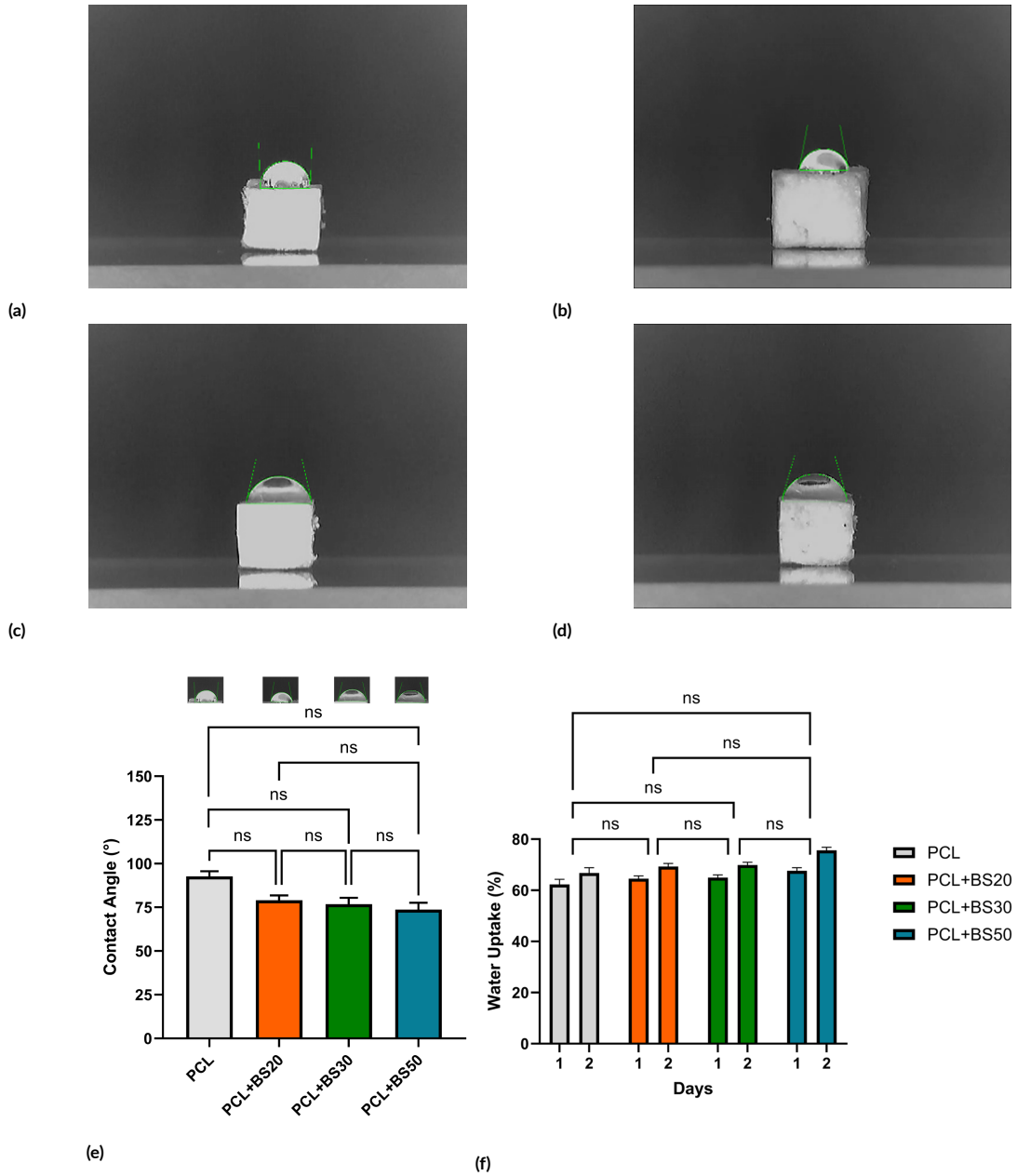

FIGURE 3 (The contact angle measurements for the scaffolds were conducted using water contact angle analysis and the angles were quantified using ImageJ for the following samples. (a) PCL. (b) PCL+BS20. (c) PCL+BS30. (d) PCL+BS50. The angle formed on the side of the water droplet. If the green line is perpendicular, then the angle formed is 90 degrees. (e) Quantification of water contact angle. (f) The water uptake for the scaffolds on day 1 and 2. ns: not significant.

test, while toxicity and proliferation can be assessed in the MTT test. Osteoinductivity means that the scaffold can induce the differentiation process of hWJ-MSCs cells into bone cells. The differentiation process was observed using the ICC test through osteogenic markers/antigen and antibody interactions and through the calcium deposition process using the Alizarin red test.

3.6. Cell morphology observation using SEM

After the seeding and growing of hWJ-MSCs on the sterile scaffold, the samples were incubated for 3 days. Subsequently, the cells attachment to the scaffold were observed based on their morphology using SEM. In Figure 4, red arrows indicate cells attachment to the surface of the scaffold, while the green arrows show the filopodia (cytoplasmic extensions) of the hWJ-MSCs. Cell morphology can be distinguished from biosilica and PCL due to the presence of nucleus and filopodia in the cytoplasm. The addition of biosilica cause the scaffold become hydrophilic, thereby supporting cell adhesion and spreading (Sundaramurthi et al. 2015; Mattila and Lappalainen 2008). Qualitatively, more hWJ-MSCs were observed adhering to the surface of the scaffold with a 50% biosilica concentration compared to the other scaffolds. This finding aligns with the results from the water contact angle and water uptake tests, which indicate that the scaffold with a 50% biosil-

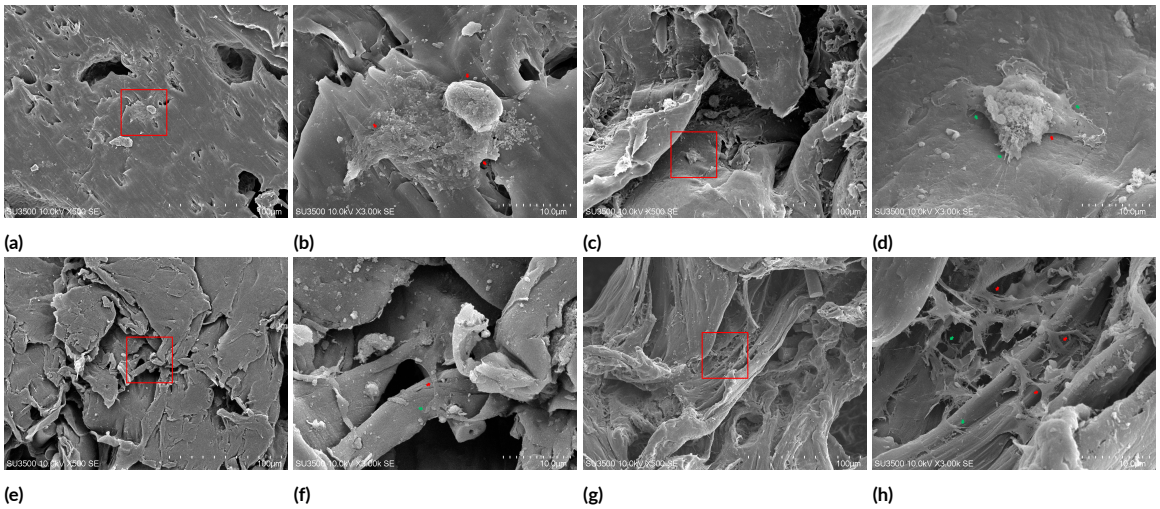

FIGURE 4 SEM observations at 500 and 3,000× magnification on the third day post-seeding. (a-b) Morphology of hWJ-MSCs passage 6 on the PCL scaffolds at (a) 500× (scale bar: 100 µm) and (b) 3,000× (scale bar: 10 µm). (c-d) Morphology of hWJ-MSCs passage 6 on the PCL+BS20 scaffolds at (c) 500x (scale bar: 100 µm) and (d) 3,000× (scale bar: 10 µm). (e-f) Morphology of hWJ-MSCs passage 6 on the PCL+BS30 scaffolds at (e) 500x (scale bar: 100 µm) and (f) 3,000× (scale bar: 10 µm). (g-h) Morphology of hWJ-MSCs passage 6 on the PCL+BS50 scaffolds at (g) 500× (scale bar: 100 µm) and (h) 3,000× (scale bar: 10 µm). Red arrows indicate cells attached to the surface of the scaffold, while the green arrows show the cytoplasmic extensions of the hWJ-MSCs.

ica concentration was the most hydrophilic. A hydrophilic environment facilitates integrin proteins to bind with the substrate. Furthermore, on the PCL scaffold, cytoplasmic extensions were not as prominently observed due to the hydrophobic nature of the scaffold, which hinders cell adhesion (Ganesh et al. 2012; Khosravi et al. 2018). Cell behavior was affected the structure and composition of the scaffold. Biosilica in scaffolds, bind to cells via several mechanism, including via integrin. The binding between scaffold and cell will change the configuration and rearrangement of cytoskeletal proteins inside the cell, such as actin It will eventually lead to the differentiation of the cell, which also known as the mechano-transduction process (Taye et al. 2024).

3.7. Cytotoxicity testing of hWJ-MSCs on the scaffold

After observing the morphology of hWJ-MSCs on the scaffold, the biocompatibility of the scaffold was tested using the MTT assay. According to Anggani et al. (2021), a scaffold is considered non-toxic to cells when the cell viability is above 70%. Based on the results obtained in Figure 5A, there are no significant differences among the variations, and all scaffold variations exhibit viability values above 70%. Therefore, it can be concluded that the scaffolds are non-toxic to hWJ-MSCs. Consequently, the cells can grow and synthesize as long as their nutritional needs are met, thereby facilitating both proliferation and differentiation (Qu et al. 2019; Shahin-Shamsabadi et al. 2018).

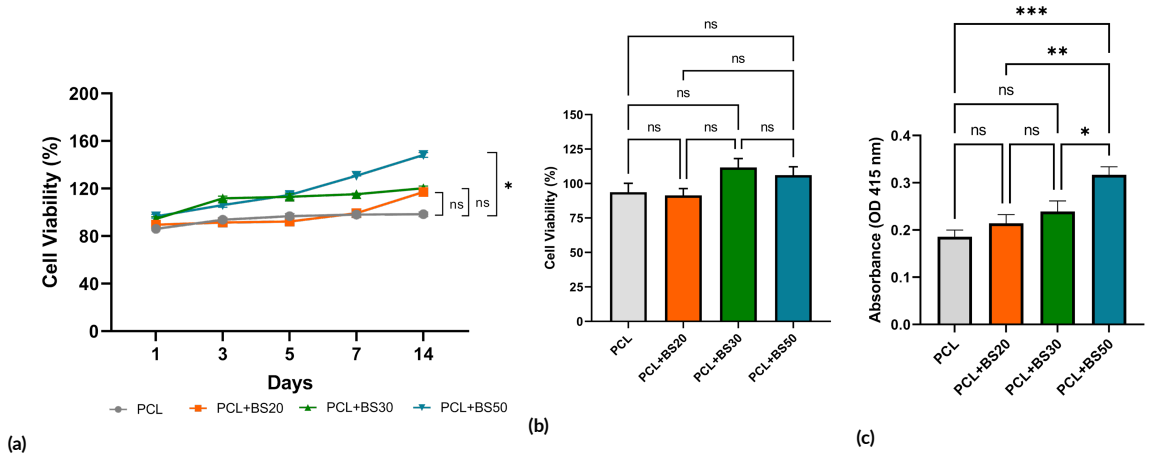

FIGURE 5 The percentage of viability of hWJ-MSCs at passage 6 on the scaffold was assessed using: (a) the cytotoxic MTT assay, (b) the proliferative MTT assay, and (c) the Alizarin Red assay. Results indicate no significant difference (ns, $p > 0.05$), whereas a significant difference is marked by an asterisk (*), * ($p \leq 0.05$), ** ($p \leq 0.01$), *** ($p \leq 0.001$).

3.8. Proliferation testing of hWJ-MSCs on the Scaffold

The proliferative MTT assay aims to determine whether the scaffold stimulates the growth of hWJ-MSCs, enabling proliferation to occur. This test was conducted over a period of 14 days, with assessments made on days 1, 3, 5, 7, and 14 post-seeding of the cells onto the scaffold. As it is shown on Figure 5b, the proliferation of hWJ-MSCs on the scaffold with a 50% biosilica concentration is significantly different compared to the PCL scaffold. This finding aligns with the results from the water contact angle and water uptake tests, which indicate that the scaffold with a 50% biosilica concentration is the most hydrophilic.

A hydrophilic environment facilitates integrin proteins to bind the scaffold. The facilitated cell adhesion ultimately supports cell proliferation and differentiation (Ganesh et al. 2012; Khosravi et al. 2018). The presence of proliferation indicates that the scaffold has mimicked the bone extracellular matrix, thereby supporting cell growth and differentiation through interactions between cells and the scaffold, as well as between cells themselves (Gandhimathi et al. 2019).

3.9. Differentiation potency of hWJ-MSCs on the scaffold

The differentiation process of hWJ-MSCs on the composite scaffold was determined using immunocytochemistry (ICC). This technique was used to detect and visualize the presence and localization of specific proteins or antigens in cells using conjugated dye antibodies that can be observed under a confocal microscope. The dyes used in this study include DAPI for staining cell nuclei, Rhodamine Phalloidin for actin filaments, primary antibody for type I collagen and osteopontin. The observations on day 21 indicate that hWJ-MSCs have differentiated into osteoblasts, indicated by the presence of type I collagen and osteopontin proteins serving as osteogenic markers at the osteoblast stage (Figure 6). The hWJ-MSCs on the PCL scaffold did not show any expression of these two markers, leading to the conclusion that the hWJ-MSCs seeded on the PCL scaffold did not differentiate into osteoblasts due to the absence of biosilica. Biosilica is osteo-inductive, thus capable of stimulating hWJ-MSCs to differentiate into bone-forming cells. This contrasts with PCL, which is biocompatible but not osteo-inductive.

Biosilica acts as an inducer both mechanically and chemically by creating an artificial bone environment due to the interaction between the Si-O groups of biosilica and various ions in the growth medium. The artificial environment mimics the extracellular matrix of bone tissue, specifically hydroxyapatite (HA), therefore when hWJ-MSCs are grown on a scaffold containing biosilica, an induction process occurs that directs the cells to differentiate (Taye et al. 2024). The ICC test is semi-qualitative, so to determine which scaffold can induce the differentiation process most effectively, other quantitative tests should be employed.

3.10. Mineralization assay of hWJ-MSCs on the scaffold

Mineralization is an important process that occurs after hWJ-MSCs differentiate into osteoblasts in the context of bone tissue formation. It is a central mechanism to the development of functional bone tissue. The osteoblasts differentiation will carry out through mineralization by depositing minerals, primarily calcium and phosphate, onto type I collagen, leading to the formation of hydroxyapatite (HA). HA is the extracellular matrix that constitutes bone tissue, along with osteocyte cells (Shi et al. 2021). One of the assays used to measure the mineralization process of hWJ-MSCs into osteoblasts is the Alizarin Red staining assay. Alizarin Red is a staining assay that has a strong affinity for calcium, one of the key minerals that make up HA, making it ideal for identifying and quantitatively measuring the mineralization process.

Figure 3c presents the results of the Alizarin Red assay for each scaffold variation. Based on the results obtained, the scaffold with a biosilica concentration of 50% exhibited the highest optical density (OD) compared to the other treatments. The OD value correlates with the calcium deposition process; the higher the OD value, the more calcium is deposited (Gandhimathi et al. 2019). The OD value recorded for the PCL scaffold represents the absorbance of the Alizarin Red dye as measured by the microplate reader, rather than calcium deposition, because the red dye from Alizarin red cannot be removed after the cell fixation and washing process (the scaffold was stained by red dye). This is substantiated by the results of the ICC assay shown in Figure 6, where in the PCL scaffold, hWJ-MSCs did not express type I collagen protein, which serves as the extracellular matrix for the calcium deposition process. The absence of type I collagen expression indicates that hWJ-MSCs did not differentiate into osteoblasts.

In addition to the expression of type I collagen protein, calcium deposition also serves as an indicator that hWJ-MSCs have differentiated. Calcium deposition aims to form the extracellular matrix of bone tissue, specifically HA, in conjunction with type I collagen (Gandhimathi et al. 2019; Shi et al. 2021). Increasing the biosilica concentration in the scaffold enhances the calcium deposition process. The amount of calcium deposited correlates with the number of hWJ-MSCs that have differentiated into osteoblasts. This is supported by the proliferation test results, showing that the scaffold with a 50% biosilica concentration achieved the highest cell viability, resulting in a correspondingly high OD value in the mineralization process (Ganesh et al. 2012; Khosravi et al. 2018). hWJ-MSCs cells do not produce calcium. The calcium deposited comes from the growth medium, which is replaced every two days during the Alizarin Red test. The replacement of the growth medium provides sufficient nutritional needs, especially calcium ions for the deposition process.

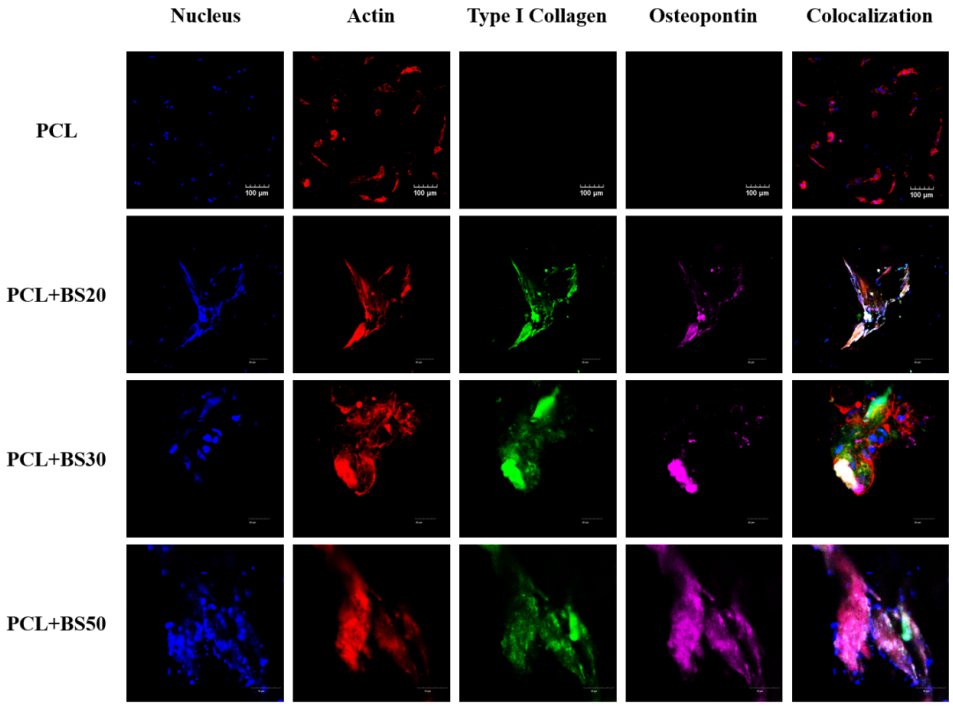

FIGURE 6 Morphology of hWJ-MSCs at passage 6 on the scaffold through ICC on day 21. From left to right: nucleus (blue fluorescent); actin filament (red fluorescent); type I collagen (green fluorescent); osteopontin (magenta fluorescent). This image was taken by confocal laser scanning FV4000 (Evident Scientific, Singapore).

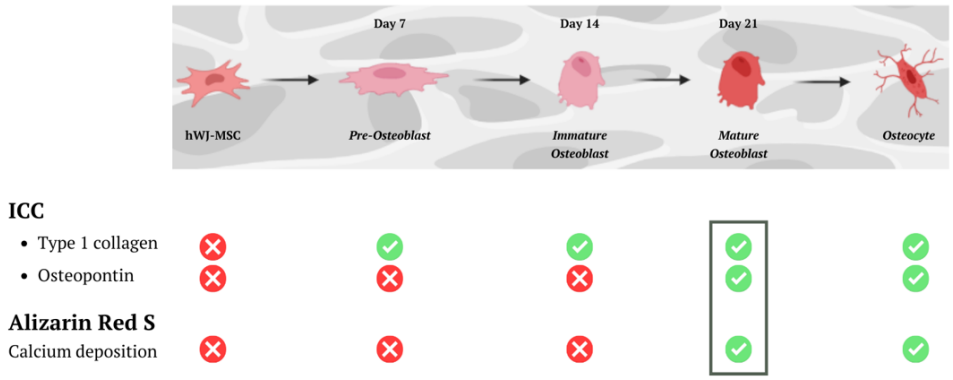

FIGURE 7 Illustration of hWJ-MSCs differentiation stages into osteocytes based on ICC and Alizarin Red tests. Figure created with BioRender.com.

3.11. Confirmation of hWJ-MSCs differentiation stages on scaffold

Based on the ICC and Alizarin Red test results, further confirmation is needed to determine whether the differentiated hWJ-MSCs are at the osteoblast or osteocyte stage Three key parameters were assessed in osteoblast differentiation process, i.e. the expression of type I collagen protein, the expression of osteopontin, and the presence of calcium deposition. The three parameters are present at the mature osteoblast and osteocytes stage. Osteocytes produce less type I collagen than osteoblasts, indicating that the differentiated hWJ-MSCs are at the osteoblast stage and have not yet progressed to osteocytes on day 21 (Selvaraj et al. 2024), referring to the ICC results in Figure 6. Osteoblasts differentiate into osteocytes when HA forms through the production of collagen type I by osteoblasts and the deposition of calcium. The formation of HA as the extracellular matrix in bone tissue traps or encases osteoblasts, leading to their differentiation into osteocytes (Gandhimathi et al. 2019).

4. Conclusions

The scaffold with 50% biosilica concentration demonstrates the most favorable properties for supporting hWJ-MSC growth, exhibiting strong mechanical strength and hydrophilic characteristics. Additionally, the scaffold enhances cell proliferation and promotes osteogenic differ-

entiation, confirmed by collagen type I and osteopontin expression and a higher OD value in the Alizarin Red assay. Thus, the 50% biosilica composite scaffold is biocompatible and osteoconductive, therefore it became a promising candidate for bone tissue engineering. Future research should focus on molecular-level gene expression analysis and *in vivo* studies to validate its effectiveness.

Acknowledgments

Special thanks to Dr. Walter Balansa and Frets Jonas Rieuwpassa, M.Si. from Politeknik Negeri Nusa Utara for providing the sponge Xestospongia testudinaria from Sangihe Islands, North Sulawesi Province. Thanks also to Evident Scientific Singapore for providing the facility for ICC test observation using the confocal laser scanning FV4000.

Authors' contributions

AA, AB, SHS designed the study. AB, CK provides resources. AA carried out the laboratory work. AA, AB, CK, SHS analyzed the data. AA wrote the manuscript. AB, CK, SHS supervising and reviewing the manuscript. All authors read and approved the final version of the manuscript.

Competing interests

The authors declare that there are no conflicts of interest related to this publication.

References

Alibrahim KA. 2022. FTIR, 1H NMR, TGA, TEM and biological studies on the new synthesized nano zirconium(iv) captopril hypertension drug complex. Farmacia 70(1):133–137. doi:10.31925/farmacia.2022.1.19.

Anggani OF, Setiya Budiatin A, Sulmartiwi L, Rahmad Royan M. 2021. *In Vitro* Cytotoxicity Test Reveals Non-toxic of Waste-based Scaffold on Human Hepatocyte Cells. J. Aquac. Fish Heal. 10(1):109–116. doi:10.20473/jafh.v10i1.23424.

Aung SW, Abu Kasim NH, Ramasamy TS. 2019. Isolation, Expansion, and Characterization of Wharton's Jelly-Derived Mesenchymal Stromal Cell: Method to Identify Functional Passages for Experiments. Methods Mol. Biol. 2045:323–335. doi:10.1007/7651_2019_242.

Barcena AJR, Mishra A, Bolinas DKM, Martin BM, Melancon MP. 2024. Integration of electrospun scaffolds and biological polymers for enhancing the delivery and efficacy of mesenchymal stem/stromal cell therapies. Front. Biosci. (Landmark Ed.) 29(6):228. doi:10.31083/j.fbl2906228.

Barros AA, Aroso IM, Silva TH, Mano JF, Duarte ARC, Reis RL. 2014. Surface modification of silica-based marine sponge bioceramics induce hydroxyapatite formation. Cryst. Growth Des. 14(9):4545–4552. doi:10.1021/cg500654u.

Beniwal G, Saxena KK. 2021. A review on pore and porosity in tissue engineering. In: Mater. Today Proc., volume 44. p. 2623–2628. doi:10.1016/j.matpr.2020.12.661.

Cannillo V, Chiellini F, Fabbri P, Sola A. 2010. Production of Bioglass® 45S5 - Polycaprolactone composite scaffolds via salt-leaching. Compos. Struct. 92(8):1823–1832. doi:10.1016/j.compstruct.2010.01.017.

Cao S, Zhao Y, Hu Y, Zou L, Chen J. 2020. New perspectives: In-situ tissue engineering for bone repair scaffold. Compos. Part B Eng. 202:108445. doi:10.1016/j.compositesb.2020.108445.

Caplan AI. 2007. Adult mesenchymal stem cells for tissue engineering versus regenerative medicine. J. Cell. Physiol. 213(2):341–347. doi:10.1002/jcp.21200.

Chaparro O, Linero I. 2016. Regenerative Medicine: A New Paradigm in Bone Regeneration. Rijeka: IntechOpen. p. 386. doi:10.5772/62523.

de Almeida Cruz M, Gabbai-Armelin PR, de França Santana A, dos Santos Prado JP, Avanzi IR, Parisi JR, Custódio MR, Granito RN, Renno ACM. 2020. *In vivo* biological effects of marine biosilica on a tibial bone defect in rats. Brazilian Arch. Biol. Technol. 63:e20190084. doi:10.1590/1678-4324-2020190084.

Dudik O, Amorim S, Xavier JR, Rapp HT, Silva TH, Pires RA, Reis RL. 2021. Bioactivity of Biosilica Obtained From North Atlantic Deep-Sea Sponges. Front. Mar. Sci. 8:637810. doi:10.3389/fmars.2021.637810.

Emadi H, Baghani M, Khodaei M, Baniassadi M, Tavangarian F. 2024. Development of 3D-Printed PCL/Baghdadite Nanocomposite Scaffolds for Bone Tissue Engineering Applications. J. Polym. Environ. 32(8):1–19. doi:10.1007/s10924-023-03156-7.

Facchin F, Bianconi E, Romano M, Impellizzeri A, Alviano F, Maioli M, Canaider S, Ventura C. 2018. Comparison of oxidative stress effects on senescence patterning of human adult and perinatal tissue-derived stem cells in short and long-term cultures. Int. J. Med. Sci. 15(13):1486. doi:10.7150/ijms.27181.

Gandhimathi C, Quek YJ, Ezhilarasu H, Ramakrishna S, Bay BH, Srinivasan DK. 2019. Osteogenic differentiation of mesenchymal stem cells with silica-coated gold nanoparticles for bone tissue engineering. Int. J. Mol. Sci. 20(20):5135. doi:10.3390/ijms20205135.

Ganesh N, Jayakumar R, Koyakutty M, Mony U, Nair SV. 2012. Embedded silica nanoparticles in poly(caprolactone) nanofibrous scaffolds enhanced osteogenic potential for bone tissue engineering. Tissue Eng. - Part A 18(18):1867–1881. doi:10.1089/ten.tea.2012.0167.

Giuliani N, Lisignoli G, Magnani M, Racano C, Bolzoni M, Dalla Palma B, Spolzino A, Manferdini C, Abati

C, Toscani D, Facchini A, Aversa F. 2013. New insights into osteogenic and chondrogenic differentiation of human bone marrow mesenchymal stem cells and their potential clinical applications for bone regeneration in pediatric orthopaedics. Stem Cells Int. p. 312501. doi:10.1155/2013/312501.

Hadi TA, Hafizt M, Hadiyanto, Budiyanto A, Siringoringo RM. 2018. Shallow water sponges along the south coast of Java, Indonesia. Biodiversitas 19(2):485–493. doi:10.13057/biodiv/d190223.

Herth E, Zeggari R, Rauch JY, Remy-Martin F, Boireau W. 2016. Investigation of amorphous SiOx layer on gold surface for Surface Plasmon Resonance measurements. Microelectron. Eng. 163:43–48. doi:10.1016/j.mee.2016.04.014.

Huang YZ, Xie HQ, Li X. 2020. Scaffolds in Bone Tissue Engineering: Research Progress and Current Applications. Elsevier. p. 204–215. doi:10.1016/b978-0-12-801238-3.11205-x.

Kalkan E, Nadaroğlu H, Celebi N, Tozsin G. 2014. Removal of textile dye Reactive Black 5 from aqueous solution by adsorption on laccase-modified silica fume. Desalin. Water Treat. 52(31-33):6122–6134. doi:10.1080/19443994.2013.811114.

Kangari P, Talaei-Khozani T, Razeghian-Jahromi I, Razmkhah M. 2020. Mesenchymal stem cells: amazing remedies for bone and cartilage defects. doi:10.1186/s13287-020-02001-1.

Khosravi A, Ghasemi-Mobarakeh L, Mollahosseini H, Ajalloueian F, Masoudi Rad M, Norouzi MR, Sami Jokandan M, Khoddami A, Chronakis IS. 2018. Immobilization of silk fibroin on the surface of PCL nanofibrous scaffolds for tissue engineering applications. J. Appl. Polym. Sci. 135(37):46684. doi:10.1002/app.46684.

Lin H, Wang X, Huang M, Li Z, Shen Z, Feng J, Chen H, Wu J, Gao J, Wen Z, Huang F, Jiang Z. 2020. Research hotspots and trends of bone defects based on Web of Science: A bibliometric analysis. J. Orthop. Surg. Res. 15(1):1–15. doi:10.1186/s13018-020-01973-3.

Marino L, Castaldi MA, Rosamilio R, Ragni E, Vitolo R, Fulgione C, Castaldi SG, Serio B, Bianco R, Guida M, Selleri C. 2019. Mesenchymal stem cells from the Wharton's jelly of the human umbilical cord: Biological properties and therapeutic potential. Int. J. Stem Cells 12(2):218–226. doi:10.15283/ijsc18034.

Mattila PK, Lappalainen P. 2008. Filopodia: Molecular architecture and cellular functions. Nat. Rev. Mol. Cell Biol. 9(6):446–454. doi:10.1038/nrm2406.

Mori G, Brunetti G, Oranger A, Carbone C, Ballini A, Muzio LL, Colucci S, Mori C, Grassi FR, Grano M. 2011. Dental pulp stem cells: Osteogenic differentiation and gene expression. Ann. N. Y. Acad. Sci. 1237(1):47–52. doi:10.1111/j.1749-6632.2011.06234.x.

Nauth A, Schemitsch E, Norris B, Nollin Z, Watson JT. 2018. Critical-Size Bone Defects: Is There a Consensus for Diagnosis and Treatment? J. Orthop. Trauma 32:S7–S11. doi:10.1097/BOT.0000000000001115.

O'Brien FJ. 2011. Biomaterials & scaffolds for tissue engineering. Mater. Today 14(3):8–95. doi:10.1016/S1369-7021(11)70058-X.

Phillipson K, Hay JN, Jenkins MJ. 2014. Thermal analysis FTIR spectroscopy of poly(ϵ-caprolactone). Thermochim. Acta 595:74–82. doi:10.1016/j.tca.2014.08.027.

Qu H, Fu H, Han Z, Sun Y. 2019. Biomaterials for bone tissue engineering scaffolds: A review. RSC Adv. 9(45):26252–26262. doi:10.1039/c9ra05214c.

Rieuwpassa FJ, Balansa W. 2022. First record of the rare *Leucetta avocado* sponge from Sangihe Islands, Indonesia. Aquat. Sci. Manag. 10(2):55–61. doi:10.35800/jasm.v10i2.48431.

Santana BP, Nedel F, Perelló Ferrúa C, e Silva RM, da Silva AF, Demarco FF, Lenin Villarreal Carreño N. 2015. Comparing different methods to fix and to dehydrate cells on alginate hydrogel scaffolds using scanning electron microscopy. Microsc. Res. Tech. 78(7):553–561. doi:10.1002/jemt.22508.

Selvaraj V, Sekaran S, Dhanasekaran A, Warrier S. 2024. Type 1 collagen: Synthesis, structure and key functions in bone mineralization. Differentiation 136:100757. doi:10.1016/j.diff.2024.100757.

Shahin-Shamsabadi A, Hashemi A, Tahriri M, Bastami F, Salehi M, Mashhadi Abbas F. 2018. Mechanical, material, and biological study of a PCL/bioactive glass bone scaffold: Importance of viscoelasticity. Mater. Sci. Eng. C 90:280–288. doi:10.1016/j.msec.2018.04.080.

Shaltooki M, Dini G, Mehdikhani M. 2019. Fabrication of chitosan-coated porous polycaprolactone/strontium-substituted bioactive glass nanocomposite scaffold for bone tissue engineering. Mater. Sci. Eng. C 105:110138. doi:10.1016/j.msec.2019.110138.

Shi H, Zhou Z, Li W, Fan Y, Li Z, Wei J. 2021. Hydroxyapatite based materials for bone tissue engineering: A brief and comprehensive introduction. doi:10.3390/cryst11020149.

Sundaramurthi D, Jaidev LR, Ramana LN, Sethuraman S, Krishnan UM. 2015. Osteogenic diferentiation of stem cells on mesoporous silica nanofibers. RSC Adv.) 5:69205–69214. doi:10.1039/C5RA07014G.

Taufik S A, Wiweko A, Yudhanto D, Rizki M, Habib P, Dirja BT, Rosyidi RM. 2022. Treatment of bone defects with bovine hydroxyapatite xenograft and platelet rich fibrin (PRF) to accelerate bone healing. Int. J. Surg. Case Rep. 97:107370. doi:10.1016/j.ijscr.2022.107370.

Taye MB, Ningsih HS, Shih SJ. 2024. Exploring the advancements in surface-modified bioactive glass: enhancing antibacterial activity, promoting angiogenesis, and modulating bioactivity. J. Nanoparticle Res. 26(2):28. doi:10.1007/s11051-024-05935-2.

Thiagarajan L, Abu-Awwad HADM, Dixon JE. 2017. Osteogenic Programming of Human Mesenchymal Stem Cells with Highly Efficient Intracellular Delivery of

RUNX2. Stem Cells Transl. Med. 6(12):2146–2159. doi:10.1002/sctm.17-0137.

Yu H, Xiao Q, Qi G, Chen F, Tu B, Zhang S, Li Y, Chen Y, Yu H, Duan P. 2022. A Hydrogen Bonds-Crosslinked Hydrogels With Self-Healing and Adhesive Properties for Hemostatic. Front. Bioeng. Biotechnol. 10:855013. doi:10.3389/fbioe.2022.855013.